Quantum nondemolition measurements of vibrational populations in ionic traps

L. Davidovich,[1] M. Orszag,[2] and N. Zagury[1]
[1]*Instituto de Física, Universidade Federal do Rio de Janeiro, Caixa Postal 68528, 21945-970 Rio de Janeiro, RJ, Brazil*
[2]*Facultad de Física, Pontificia Universidad Católica de Chile, Casilla 306, Santiago, Chile*
(Received 3 April 1996)

We discuss a simple implementation of a quantum nondemolition measurement of the vibronic state of a trapped ion. This scheme allows the production of Fock states associated to the center-of-mass motion and the determination of the population distribution of the trap levels, and is based on the vibronic level dependence of the frequency of Rabi oscillations between two internal states of the ion, induced by a resonant carrier field. The same scheme can be used to produce a Schrödinger-cat-like state after a single interaction between the trapped ion and the carrier pulse, followed by the detection of the ionic internal state.
[S1050-2947(96)09511-X]

PACS number(s): 42.50.Vk, 42.50.Lc, 42.50.Dv, 03.65.Bz

I. INTRODUCTION

Recent advancements in ionic and atomic traps [1–5] and in cavity quantum electrodynamics (QED) [6] have motivated the realization of experiments which demonstrate fundamental features of quantum mechanics. The attainment of low temperatures and low-dissipation regimes has allowed the investigation of single quantum systems, and the realization of basic models of quantum optics, which contemplate the interaction between bosons and a two-level system [7,8]. In cavity QED, two atomic levels are strongly coupled with a mode of a high-Q cavity, either in the optical [9,10] or in the microwave region [6,11–13]. In ion traps, two electronic levels are coupled either by a direct transition [2,14] or via a third virtual level, through a nonresonant Raman stimulated transition with two optical fields [5,15–18]. The bosons correspond to the center-of-mass motion in the approximately harmonic potential produced by the trapping electromagnetic fields.

Single trapped ions have led to the observation of quantum jumps [14] and of antibunching and sub-Poissonian behavior [19] in resonance fluorescence, and to the demonstration of the quantum Zeno effect [20], while cavity QED experiments have led to the observation of spontaneous emission inhibition [22], collapses and revivals [23], and the vacuum Rabi splitting [10,11]. The realization of quantum logic gates with laser-cooled trapped ions has been proposed by Cirac and Zoller [21] and demonstrated experimentally [17]. Several proposals have been presented for the realization of experiments which would lead to nonclassical states of the electromagnetic field or of the atomic center-of-mass oscillations. They include the generation of Fock states of the electromagnetic field in cavities [12] or of the center-of-mass motion of an atom in a trap [24], or yet the production of squeezed states of motion [15,25,26] or squeezed atomic states [27], which could be used for improving frequency standards. A recent experiment has led to the creation of Fock, coherent, and squeezed states of motion of a harmonically bound $^{9}Be^{+}$ ion [18].

Furthermore, it has been shown that cavity QED offers an appropriate environment for the realization of quantum nondemolition (QND) measurements [12], proposed originally by Braginsky *et al.* [28] as sensitive probes of gravitational waves. Cavity QED may also lead to tests of decoherence theory [29,30], which is at the core of the quantum theory of measurement [31].

Quantum nondemolition measurements are designed to avoid the ''back action'' of the measurement on the detected observable. They have been implemented in the optical domain [32], via some kind of Kerr effect in a solid or gaseous medium. The signal field to be measured interacts nonlinearly with a probe field whose phase changes by a quantity which depends on the number of photons in the signal beam. The nonlinear character of the interaction requires a relatively intense signal beam. Reference [12] proposes a QND method to measure the number of photons stored in a high-Q cavity, which is sensitive to a very small number of photons. It is based on the detection of the dispersive phase shift produced by the field on the wave function of nonresonant atoms crossing the cavity. This shift, which is proportional to the photon number in the cavity, is measured by atomic interferometry, using the Ramsey separated-oscillatory-field method. Since the atoms are nonresonant, no photon is exchanged between them and the cavity, and the measurement is indeed a QND one. However, the information acquired by detecting a sequence of atoms modifies the state of the field step by step, until it eventually collapses into a Fock state, which is *a priori* unpredictable. Repetition of the measurement for the same initial state of the field will yield a distribution of Fock states, which reproduces the initial distribution of the field.

In this paper, we show that it is possible to realize a QND measurement of the vibrational population distribution for an ion in a Paul trap [33]. As in the cavity QED proposal, a Fock state is generated in the process. Even though this Fock state is *a priori* unpredictable, it becomes completely known once the sequence of measurements is completed. Also, when applied to an initial coherent vibrational state, the first step of the measuring sequence may produce a quantum superposition of two well-separated coherent states, which is an example of a ''Schrödinger cat state.'' States of this kind have been recently demonstrated by the NIST group [34], who prepared a superposition of spatially separated coherent harmonic oscillation states of the center-of-mass of a trapped

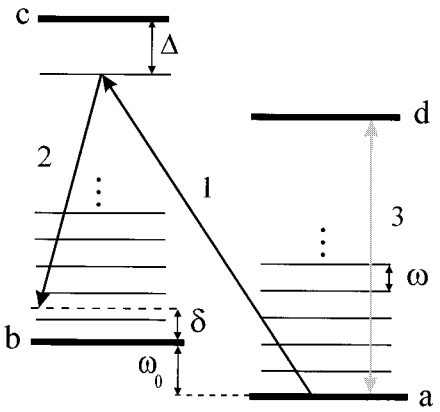

FIG. 1. Energy level diagram for the QND measurement scheme. A Raman stimulated transition is induced between levels $|a\rangle$ and $|b\rangle$ by laser beams 1 and 2. Detection of the electronic state is provided by the scattered photons resulting from the cycling transition $|a\rangle \leftrightarrow |d\rangle$, produced by the resonant pulse 3.

$^9Be^+$ ion. Their method involves a sequence of interactions of the atomic ion with laser pulses of different frequencies and areas. In contrast, our proposal leads to a Schrödinger cat state after a single interaction, followed by detection. Although it is possible to use for ionic traps a procedure similar to the QND method suggested for cavity QED, we propose here a much simpler approach.

The model on which our discussion is based is introduced in Sec. II. The QND measurement scheme is explained in Sec. III. Numerical examples are shown in Sec. IV, while the results are summarized in Sec. V.

II. MODEL

The basic level scheme is illustrated in Fig. 1 [5,16]. The electronic states $|a\rangle$ and $|b\rangle$, assumed to be metastable (they will be typically two ground state hyperfine sublevels, coupled by quadrupole transitions), and separated by an energy $\hbar\omega_0$, are coupled by a stimulated Raman transition via two optical fields (treated here as classical fields) $\vec{E}_i = \vec{E}_{0i}[e^{i(\vec{k}_i\cdot\vec{x}-\omega_i t+\phi_i)} + \text{c.c.}]$, $i=1,2$, $\vec{E}_{0i}$ real, where $\vec{x}$ is the operator associated with the center-of-mass position of the ion, and with $\omega_1-\omega_2=(k_1-k_2)c=\omega_0+\delta$, δ being a detuning of the order of the vibrational frequencies of the ion. Both fields are detuned from the electric dipole transitions from $|a\rangle$ and $|b\rangle$ to a third level $|c\rangle$, assumed to have lifetime γ^{-1}. A fourth level $|d\rangle$ is used for detecting the electronic state of the ion, and also for Doppler precooling. We assume that the ion is trapped in a harmonic potential. In the experiment described in Ref. [34], $|a\rangle$ is the $^2S_{1/2}(F=2,\ m_F=-2)$ hyperfine ground state of a $^9Be^+$ trapped ion, $|b\rangle$ corresponds to the state $^2S_{1/2}(F=1,\ m_F=-1)$, $|c\rangle$ is the state $^2P_{1/2}(F=2,\ m_F=-2)$, and $|d\rangle$ is the state $^2P_{3/2}(F=3,\ m_F=-3)$.

Each Cartesian component of the center-of-mass position operator, denoted by x_i, can be expressed in terms of lowering and raising operators a_i and $a_i^\dagger$ in the following way:

$$x_i=\left(\frac{\hbar}{2m\omega_i}\right)^{1/2}(a_i+a_i^\dagger), \tag{1}$$

where ω_i is the frequency of oscillations along the direction i.

The Hamiltonian which describes the evolution of the system between detections (so that level $|d\rangle$ does not participate in the dynamics) can be written as (choosing the energy of the state $|a\rangle$ as zero)

$$H=H_0+H_1, \tag{2}$$

where

$$H_0=\sum_{i=x,y,z}\hbar\omega_i a_i^\dagger a_i+\hbar\omega_0|b\rangle\langle b|+\hbar\omega_c|c\rangle\langle c|, \tag{3}$$

and

$$H_1=\hbar g_1 e^{-i(\vec{k}_1\cdot\vec{x}-\omega_1 t+\phi_1)}|a\rangle\langle c| + \hbar g_2 e^{-i(\vec{k}_2\cdot\vec{x}-\omega_2 t+\phi_2)}|b\rangle\langle c|+\text{H.c.} \tag{4}$$

This Hamiltonian has been written under the optical rotating wave approximation, which implies that the transitions from $|c\rangle$ to $|a\rangle$ and $|b\rangle$ are coupled with the negative-frequency parts of the fields $\vec{E}_1$ and $\vec{E}_2$, respectively. The phases of states $|a\rangle$, $|b\rangle$, and $|c\rangle$ are chosen so that the coupling constants g_1 and g_2 are real and positive (alternatively, one may incorporate these phases into the definitions of ϕ_1 and ϕ_2). These constants, which represent half the Rabi frequencies associated with the $|a\rangle\leftrightarrow|c\rangle$ and $|b\rangle\leftrightarrow|c\rangle$ transitions, are given by $g_i=\vec{d}_i\cdot\vec{E}_{0i}/\hbar$, where $\vec{d}_1$ and $\vec{d}_2$ are the electric dipole matrix elements corresponding to the transitions $|a\rangle\leftrightarrow|c\rangle$ and $|b\rangle\leftrightarrow|c\rangle$, respectively.

The linewidths of levels $|a\rangle$ and $|b\rangle$ are assumed to be much smaller than the frequencies ω_i (this corresponds to the resolved sideband limit). We take as infinite the lifetime of the vibrational modes (in actual experiments [16,34], lifetimes of the order of milliseconds have been obtained — this time scale is much larger than those involved in the present method, as will be shown in the following).

In the limit in which the magnitude of Δ, defined as $\omega_c-\omega_1$, is much larger than γ, $|\delta|$, g_1, and g_2, the state $|c\rangle$ can be adiabatically eliminated [15,27], and an effective Hamiltonian can be written for the states $|a\rangle$ and $|b\rangle$ (it is easy to show that this Hamiltonian yields the amplitude equations derived in Ref. [27]):

$$H_{\text{eff}}=H_0'+H_I, \tag{5}$$

where

$$H_0'=\sum_{i=x,y,z}\hbar\omega_i a_i^\dagger a_i-\hbar\delta'\sigma_3, \tag{6}$$

and

$$H_I=-\frac{\hbar\Omega_0}{2}[\sigma_+ e^{-i(\delta\vec{k}\cdot\vec{x}+\phi)}+\text{H.c.}]. \tag{7}$$

In these equations, $\delta\vec{k}=\vec{k}_2-\vec{k}_1$, $\phi=\phi_2-\phi_1$, and $\sigma_3=(|b\rangle\langle b|-|a\rangle\langle a|)/2$, $\sigma_+=|b\rangle\langle a|$ are the usual Pauli spin operators. For the Raman stimulated transition scheme, Ω_0 can be expressed in terms of Δ and the frequencies g_1 and

g_2: $\Omega_0 = 2g_1 g_2/\Delta$. The frequency $\delta' = \delta - g_1^2/\Delta + g_2^2/\Delta$ differs from the previously defined detuning δ by the Stark shifts of states $|a\rangle$ and $|b\rangle$.

A similar Hamiltonian is obtained if the transition between the states $|1\rangle$ and $|2\rangle$ is directly stimulated by a single classical field. In this case, $-\hbar\delta'$ should be replaced by the energy difference between the two levels, and Ω_0 would be the Rabi frequency associated to the interaction with that field [8]. Even though our discussion applies equally well to this situation, we prefer to concentrate on the Raman stimulated case, which is of wider applicability [15,16].

For the experiment described in Ref. [16], the oscillation frequencies along x, y, and z are in the range $10-30$ MHz, $\omega_0/2\pi \approx 1.250$ GHz, $\Delta/2\pi \approx 12$ GHz, $\gamma/2\pi \approx 20$ MHz, and $\Omega_0/2\pi$ is of the order of 1 MHz.

Defining as usual the Lamb-Dicke parameters $\eta_i = \delta k_i (\hbar/2m\omega_i)^{1/2}$, so that η_i^2 is the ratio between the recoil energy and the vibrational quantum of energy in the i direction (in the experiment reported in Ref. [16], $|\eta_i|$ ranges from 0.1 to 0.2, approximately), we may write H_I in the interaction picture as follows:

$$H_I^{\rm int} = -\frac{\hbar\Omega_0}{2}\left\{\sigma_+ \exp\left[-i\sum_j \eta_j (a_j e^{-i\omega_j t} + a_j^\dagger e^{i\omega_j t})\right] \times \exp(-i\delta' t)\exp(-i\phi) + \text{H.c.}\right\}. \tag{8}$$

For a Raman stimulated transition resonant with the kth vibrational red sideband in the i direction, one has $\delta' = -k\omega_i$, $k>0$. One can then conserve in the Hamiltonian (8) only the time-independent terms. Assuming for simplicity that only vibrations in the direction ℓ are excited (this will be the case if ω_ℓ is different from the other ω_i's, or if $\vec{\delta k}$ is along the direction ℓ), one is led to the Hamiltonian [36] (the index ℓ is suppressed in the following, since only one vibrational mode is involved)

$$H_I^{\rm int} = -\frac{\hbar\Omega_0}{2}[f_k(a^\dagger a)\sigma_+ a^k e^{-i\phi} + \text{H.c.}], \tag{9}$$

where the normally-ordered form of $f_k(a^\dagger a)$ is given by (cf. Ref. [36] for a similar result derived for a standing wave)

$$f_k(a^\dagger a) = f_k^{(n)}(a^\dagger a) = e^{-\eta^2/2}\sum_{\ell=0}^{\infty} \frac{(-i\eta)^{2\ell+k}}{\ell!(\ell+k)!}(a^\dagger)^\ell a^\ell. \tag{10}$$

Equation (9) corresponds to a generalized Jaynes-Cummings Hamiltonian, involving multiquantum transitions (if instead $\delta' = k\omega_i$, again with $k>0$, one gets a ''counter-rotating'' Hamiltonian). In particular, if $k=1$ and $|\eta|\sqrt{n} \ll 1$ for all relevant excitation numbers n (Lamb-Dicke limit [35]), one can approximate the sum in Eq. (10) by its first term, so that, up to first order in η, we get

$$H_I^{\rm int} = \frac{i\hbar\Omega_0\eta}{2}\sigma_+ a + \text{H.c.}, \tag{11}$$

which corresponds to the usual Jaynes-Cummings Hamiltonian [7].

From Eq. (11) we can see that if $\delta = \omega + \nu$, with ν much smaller than ω, and at the same time much larger than the electronic linewidth and the second-order ac Stark shift $\Omega_0^2\eta^2 n/\nu$, where n is any relevant vibrational occupation number, one reproduces, in the Lamb-Dicke limit, the conditions of dispersive interaction considered in the QND proposal of Ref. [12]. This implies that similar procedures can be applied to this case. We refrain, however, from analyzing this situation in detail, since a much simpler QND method can be envisaged for the system here considered.

III. QND MEASUREMENT SCHEME

Our proposal is based on the situation in which the Raman transition is precisely resonant with the Stark-shifted electronic levels, that is, $\delta' = 0$. One has then

$$H_I^{\rm int} = -\frac{\hbar\Omega_0}{2}[f_0(a^\dagger a)\sigma_+ e^{-i\phi} + \text{H.c.}], \tag{12}$$

with

$$\Omega_n \equiv \Omega_0\langle n|f_0(a^\dagger a)|n\rangle = \Omega_0\langle n|e^{-i\eta(a+a^\dagger)}|n\rangle = \Omega_0 e^{-\eta^2/2}L_n(\eta^2), \tag{13}$$

where $L_n(\eta^2)$ is the Laguerre polynomial of order n:

$$L_n(x) = \sum_{\ell=0}^{n}\binom{n}{n-\ell}\frac{(-x)^\ell}{\ell!}. \tag{14}$$

The Hamiltonian (12) leads to Rabi oscillations between the electronic levels $|a\rangle$ and $|b\rangle$, without affecting the vibrational quantum numbers. The Rabi frequency depends, however, on the motional state. Up to fourth order in η, we have

$$\Omega_n = \Omega_0[1 - (n+\tfrac{1}{2})\eta^2 + \tfrac{1}{4}(n^2 + n + \tfrac{1}{2}\eta^4) + O(\eta^6)]. \tag{15}$$

From Eqs. (12) and (13) it follows that, if the initial state of the system is

$$|\Psi(0)\rangle = |a\rangle\sum_{n=0}^{\infty} c_n|n\rangle, \tag{16}$$

then the state at time t will be

$$|\Psi_a(t)\rangle = \sum_{n=0}^{\infty} c_n\left[|a\rangle\cos\left(\frac{\Omega_n t}{2}\right) + |b\rangle i e^{-i\phi}\sin\left(\frac{\Omega_n t}{2}\right)\right]|n\rangle, \tag{17}$$

while if the ion is initially in the electronic state $|b\rangle$, the state at time t will be

$$|\Psi_b(t)\rangle = \sum_{n=0}^{\infty} c_n\left[|a\rangle i e^{i\phi}\sin\left(\frac{\Omega_n t}{2}\right) + |b\rangle\cos\left(\frac{\Omega_n t}{2}\right)\right]|n\rangle. \tag{18}$$

The dependence of the Rabi frequency Ω_n on the occupation number n is the basis of our QND scheme, which proceeds as follows. The ion is submitted to a Raman pulse of dura-

tion τ, resonant with the electronic transition, so that the vibrational state does not change. The time τ is assumed to be much smaller than the lifetimes of states $|a\rangle$ and $|b\rangle$, and the vibrational state lifetime. Right after the pulse, the electronic state of the ion is detected, by following the stimulated excitation with a circularly polarized light pulse (σ_-, for the example mentioned above, corresponding to the levels chosen in Ref. [34]) tuned to the $|a\rangle \leftrightarrow |d\rangle$ resonance. We assume that the area of this pulse is sufficiently large so that, during this last step, the photons scattered by the ion can be detected with efficiency close to one, thus allowing one to determine the electronic state of the ion. A fluorescent signal projects the ion into the state $|a\rangle$, while the absence of fluorescence projects it in state $|b\rangle$. Note that, in the Lamb-Dicke limit, each photon-scattering event leads to negligible recoil. However, if many photons are scattered during this detection process (the detection procedure reported in Ref. [16] involves thousands of photons), appreciable heating might result even in the Lamb-Dicke limit, thus spoiling the QND procedure. If ΔE is the recoil energy due to a single scattering process, one must assume therefore that the number N of scattered photons is such that $N\Delta E \ll \hbar\omega_i$, or yet, since $\eta^2 \approx \Delta E/\hbar\omega_i$, $N \ll \eta^{-2}$. For $|\eta| \approx 0.1$, this yields $N \ll 100$. On the other hand, for a saturating cycling process, $N \approx \Gamma T/2$, where Γ is the width of level $|d\rangle$ and T the duration of the detection pulse. One must have therefore $T \ll 200/\Gamma$, which yields, for $\Gamma/2\pi \approx 20$ MHz, the upper limit $T \ll 2$ μs. Under these conditions, heating can be neglected (weaker conditions are obtained if the detection transition corresponds to a smaller Lamb-Dicke parameter), and

$$|\psi_\epsilon^{(1)}\rangle = \frac{\Sigma_{n=0}^{\infty} c_n \sin\left(\frac{\Omega_n \tau}{2} + \epsilon\frac{\pi}{2}\right)|n\rangle}{\left[\sum_{n=0}^{\infty} |c_n|^2 \sin^2\left(\frac{\Omega_n \tau}{2} + \epsilon\frac{\pi}{2}\right)\right]^{1/2}}, \tag{19}$$

where $\epsilon = 1$ if the detected electronic state coincides with the initial electronic state, and $\epsilon = 0$ otherwise.

Equation (19) shows that the original vibrational distribution is modulated by an oscillating function of n, that is,

$$P_\epsilon^{(1)}(n) = \frac{\sin^2\left(\frac{\Omega_n \tau}{2} + \epsilon\frac{\pi}{2}\right) P(n)}{\sum_{n'=0}^{\infty} \sin^2\left(\frac{\Omega_{n'} \tau}{2} + \epsilon\frac{\pi}{2}\right) P(n')}. \tag{20}$$

This implies a decimation of some of the populations, depending on the value of $\theta(\tau) \equiv \Omega_0 \eta^2 \tau/2$ [cf. Eq. (15)]. In order to enhance the dependence of Ω_n with n, we choose the duration τ of the Raman pulses so that $\theta(\tau)$ is of the order of π. For typical values of $\Omega_0/2\pi \approx 1$ MHz, $\eta \approx 0.1$, this implies $\tau \approx 50$ μs. This is by far the largest time in the cycle (since the detection process, as discussed above, should involve a pulse shorter than 1 μs), so that the duration of the whole cycle is of the order of 50 μs. Under these conditions, and if the relevant occupation numbers are smaller than 10, the term of order η^4 in Eq. (15) will give a contribution smaller than 3% of the term proportional to η^2. On the other hand, the term independent of η in Eq. (15), given by $\Omega_0 \tau$, will be about 100 times larger than the term of order η^2. This will not spoil the QND procedure, however, due to the fact that this larger contribution is independent of n, and represents therefore a phase which just displaces the fringes modulating the original distribution.

After the first sequence of Raman stimulated emission and detection, a new cycle is initiated. By changing for each run the Raman pulse area $\Omega_0 \tau$, one multiplies successively the population distribution by sines or cosines with changing periods and changing phases, so that after the ith cycle one has

$$P_\epsilon^{(i)}(n) = \frac{\sin^2\left(\frac{\Omega_n \tau_i}{2} + \epsilon\frac{\pi}{2}\right) P^{(i-1)}(n)}{\sum_{n'=0}^{\infty} \sin^2\left(\frac{\Omega_{n'} \tau_i}{2} + \epsilon\frac{\pi}{2}\right) P^{(i-1)}(n')}, \tag{21}$$

where τ_i is the duration of the Raman pulse in the ith cycle, and $P^{(i-1)}(n)$ is the probability distribution of vibronic excitations in the previous cycle [we define $P^{(0)}(n) \equiv P(n)$].

As our numerical simulations will show, this may result in the decimation of more and more populations, until finally a Fock state is reached, within a very good approximation, and the vibrational state does not change anymore. This procedure can be followed for all three directions, thus generating a three-dimensional Fock state.

It is clear that this process depends on the random nature of the electronic state detection, and therefore the Fock state to be obtained cannot be predicted *a priori*. However, if the vibronic excitation distribution becomes negligible after a finite value of n, then one is able to assert precisely the Fock state which was obtained, once the sequence of detected states and the Raman pulse durations are known. Under these conditions, this state depends only on the sequence of measurements (atomic states and pulse areas), and is independent of the initial distribution. Note that in an experiment this can be implemented in real time by feeding a computer with the data about the successive state detections and pulse durations, during an experimental run.

Furthermore, the distribution of Fock states after many realizations, starting with the same initial vibrational state, reproduces the initial distribution. Indeed, summing up over all possibilities of detection of the ion internal states is equivalent to not detecting them. Since the interaction does not change the vibrational state, the distribution should not change in this case. This can be seen explicitly in the following way. The probability $\mathcal{P}_\epsilon^{(i)}$ of detecting the ion in states $|a\rangle$ or $|b\rangle$ at the end of the ith cycle is

$$\mathcal{P}_\epsilon^{(i)} = \sum_{n=0}^{\infty} \sin^2\left(\frac{\Omega_n \tau_i}{2} + \epsilon\frac{\pi}{2}\right) P^{(i-1)}(n), \tag{22}$$

where, as before, $\epsilon = 1$ or 0 depending on whether this state coincides or not with the electronic state in the beginning of the cycle. Averaging $P_\epsilon^{(i)}(n)$ given by Eq. (21) over the

distribution $\mathcal{P}_\epsilon^{(i)}$ one gets $P^{(i)}(n)=\Sigma_{\epsilon=0,1}P_\epsilon^{(i)}(n)\mathcal{P}_\epsilon^{(i)}=P^{(i-1)}(n)$. In the same way, we show that $P^{(i-1)}(n)=P^{(i-2)}(n)=\cdots=P(n)$.

Experimental verification of the produced Fock state can be made in the following way. One repeats the experiment several times, and one selects the groups of experiments characterized by the same sequence of electronic state detections, changing, however, in the final step the pulse area so that θ spans some cycles, and measuring for each group and for each value of θ the probabilities $P_a(\theta)$ and $P_b(\theta)$ of detecting the ion in states $|a\rangle$ or $|b\rangle$. According to Eq. (15), one has in the Lamb-Dicke limit

$$\frac{\Omega_n\tau}{2}=\Phi(n,\tau)+O(\theta n^2\eta^2), \tag{23}$$

where

$$\Phi(n,\tau)=\frac{\Omega_0\tau}{2}-\frac{\theta}{2}-\theta n. \tag{24}$$

Choosing a sequence of values of the pulse area so that $\Phi(0,\tau)=(1-\eta^2/2)\Omega_0\tau/2$ is always a multiple of π (since $\Omega_0\tau\approx 200\theta$, this would still provide about 100 values for θ in a π interval), one gets for P_a and P_b sines or cosines which oscillate, as functions of θ, with frequency n. Measurement of this frequency leads therefore to the Fock state obtained in a specific realization.

The above treatment, developed for an initial pure state, can be easily generalized to statistical mixtures. Populations will still change according to Eq. (21), while the change in the density matrix elements after the ith cycle is given by

$$\rho_{n,n',\epsilon}^{(i)}=\frac{\sin\left(\frac{\Omega_n\tau_i}{2}+\epsilon\frac{\pi}{2}\right)\sin\left(\frac{\Omega_{n'}\tau_i}{2}+\epsilon\frac{\pi}{2}\right)}{\sum_m P^{(i-1)}(m)\sin^2\left(\frac{\Omega_m\tau_i}{2}+\epsilon\frac{\pi}{2}\right)}\rho_{n,n'}^{(i-1)}, \tag{25}$$

where ϵ has the same definition as before. It is clear that $|\rho_{n,n',\epsilon}^{(i)}|\leq|\rho_{n,n'}^{(i-1)}|$, so coherence will tend to be reduced, as the QND measurement progresses. If the atomic state is not detected, on the other hand, the change in the density matrix elements will be the weighted average of the expressions given by Eq. (25), the weights being the probabilities of getting each state [denominators in Eq. (25)]. We get then

$$\rho_{n,n'}^{(i)}=\cos\left(\frac{\Omega_n-\Omega_{n'}}{2}\tau_i\right)\rho_{n,n'}^{(i-1)}, \tag{26}$$

confirming that the populations do not change, while the coherences get reduced.

In practice, the whole process should take a time smaller than the decay time of the electronic or vibrational levels. In fact, as we are going to show in the following section, a few cycles are enough to produce a Fock state, if only the lowest vibrational levels are significantly populated. This implies that the whole process should take place in a time shorter than one millisecond.

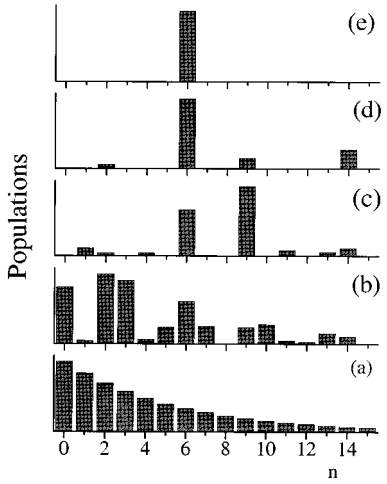

FIG. 2. Population distributions as a function of the vibronic excitation number, for a Lamb-Dicke parameter $\eta=0.1$: (a) before the first cycle, for a thermal distribution with $\langle n\rangle=5$; (b) after the first cycle; (c) after the fifth cycle; (d) after the tenth cycle; (e) after the thirteenth cycle. The pulse areas $\Omega_0\tau$ were chosen at random, so that $\theta\equiv\Omega_0\tau\eta^2/2$ remains in the interval $(1/12\pi,11/12\pi)$. Which level is detected in a given cycle was chosen according to the probability distribution given by Eq. (22).

IV. NUMERICAL RESULTS

All the following numerical simulations correspond to initial states with an average number of vibrational quanta equal to five. Both a thermal and a coherent initial state are considered. All the simulations are done in the Lamb-Dicke limit, with $\eta\approx 0.1$. We also assume that the uncertainty in the determination of the area of the Raman pulses is of the order of 10^{-4} of the area, which seems to be realistic from the experimental point of view. This precision is not necessary for getting a Fock state. It is required, however, for assessing which Fock state is obtained after a sequence of measurements.

The convergence of the distribution to a Fock state depends on the strategy adopted in the choice of the Raman pulse areas for the successive cycles (strategies for speeding up the convergence in cavity QED nondemolition measurements were discussed in Ref. [37]). We first consider simulations where we vary the Raman pulse areas at random in an interval such that $\pi/12<\theta<11\pi/12$. Which electronic level is detected at the end of each cycle is chosen according to the *a priori* probability, $\mathcal{P}_\epsilon$, given in Eq. (22), of detecting it.

We have done several simulations starting with a thermal and with a coherent state. In most of these simulations we achieved convergence to a Fock state after 18 cycles. A typical example is shown in Fig. 2.

A much faster convergence may be achieved if we could change both the phase $\Phi(0,\tau)$ and the fundamental frequency $\theta(\tau)$ at will after each cycle. In fact, once we have fixed the value of η during a real experiment, we may only change the pulse area, between cycles, which means that after each cycle the ratio between $\Phi(0,\tau)$ and $\theta(\tau)$ is maintained fixed and equal to its initial value. We may take advantage, however, of the fact that $\Phi(0,\tau)$ is experimentally much larger than π, to change the argument of the trigonometric functions that appear in Eq. (20) by a factor of

$O(\pi)$ through a small relative change in the pulse area. This small change affects the value of θ only by a factor of $O(\eta^2)$. Therefore from a practical point of view we may assume that these changes affect the phase $\Phi(0,\tau)$, but not the value of θ.

Consider that the first cycle has duration τ_0 and that we have adjusted the values of η and the initial value of $\Omega_0 t_0$ in such a way that $\Phi_0 \equiv \Phi(0,\tau_0) = (K+\kappa)\pi$, where $K \gg 1$ and $\kappa = 0$ or 1/2. We also assume that K is divisible by small integers, say $j = 2,3,4,5\ldots$, so that $\Phi(0,\tau_j) = \Phi_0 \tau_j / \tau_0$, where $\tau_j = \tau_0 / j$ is still a multiple of π plus $\kappa\pi$.

Therefore, if $\kappa = 0$ and $\theta_j \equiv \theta(\tau_0)\tau_j/\tau_0 = \pi/(2j)$, detection of the electronic level $|a\rangle$ decimates populations corresponding to n's equal to odd multiples of j, while detection of the electronic level $|b\rangle$ decimates populations corresponding to n's equal to even multiples of j, including $n = 0$. On the other hand, if $\kappa = 1/2$ and $\theta = \pi/(2j)$, detection of the electronic level $|b\rangle$ decimates populations associated with n's equal to odd multiples of j, while detection of the electronic level $|a\rangle$ decimates populations with n's equal to even multiples of j. Using these results it is easy to plan a strategy to obtain fast convergence to a Fock state when the initial average vibrational occupation number is small, using an electronic feedback mechanism to change conveniently the value of the pulse area such that θ takes one of the values $\pi/(2j)$, depending on which electronic level was detected in the previous cycle.

As an example, assume that initially the vibrational distribution is limited to occupation numbers $n \leqslant 5$, and that the internal electronic state is $|a\rangle$. In the first cycle one takes $\theta = \pi/2$ and $\kappa = 0$. After detection of the electronic level only the even ($n = 0,2,4$) or odd ($n = 1,3,5$) populations survive, depending on whether level $|a\rangle$ or $|b\rangle$ has been measured, respectively. If $|a\rangle$ is detected, one changes θ to $\pi/4$. After the second cycle, detection of level $|b\rangle$ produces a Fock state with $n = 2$, while detection of level $|a\rangle$ reduces the distribution to occupation numbers $n = 0,4$. In this last case θ is changed to $\pi/8$. Now detection of $|a\rangle$ produces the Fock state with $n = 0$ while detection of $|b\rangle$ produces the state $|4\rangle$. On the other hand, if in the first cycle level $|b\rangle$ is detected, θ should be changed to $\pi/4$ and κ to 1/2. Detection of level $|b\rangle$ reduces the distribution to populations with $n = 1$ and 5, while detection of level $|a\rangle$ generates the Fock state $|3\rangle$. In the first case one changes θ to $\pi/8$. Detection of level $|b\rangle$ generates the state $|1\rangle$ while detection of level $|a\rangle$ generates the state $|5\rangle$. In this simple example we show that choosing conveniently the pulse areas we may generate a Fock state after detection of only two or three atoms. Of course more cycles are needed if the initial distribution has a larger width. Note that our arguments depend only on the maximum number of vibronic excitations being equal to five, and not on the specific form of the distribution.

Even if the number of vibronic excitations is not limited, it is still possible to get Fock states within a very good approximation, and with fast convergence, as long as similar strategies are followed for the choices of the successive pulse areas. In Figs. 3 and 4 we show simulations of experiments where we start either with a thermal or a coherent vibrational state with $\langle n\rangle = 5$, the electronic level being $|a\rangle$, and adjust the values of η and the area of the Raman pulse in the first cycle so that $\Phi_0 = 48\pi$ and $\theta = \pi/2$. In these simulations a probability distribution very close to that corresponding to a Fock state with $n = 4$ is reached after only three or four cycles corresponding to the sequence of values $\pi/2$, $\pi/4$, $\pi/8$, $\pi/12$ for θ and the sequence of detections of the electronic levels in the (lower, lower, upper, lower) states.

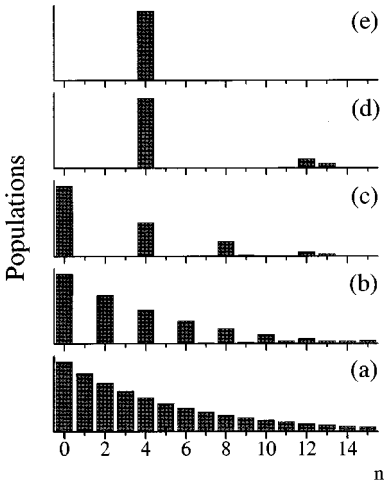

FIG. 3. Population distributions as a function of the vibronic excitation number, for $\Phi_0 = 48\pi$ and $\theta = \pi/2$ in the first cycle (Lamb-Dicke parameter $\eta \approx 0.102$: (a) before the first cycle, for a thermal distribution with $\langle n\rangle = 5$; (b) after the first cycle ($\theta = \pi/2$, lower level detected); (c) after the second cycle $\theta = \pi/4$, lower level detected); (d) after the third cycle ($\theta = \pi/8$, upper level detected); (e) after the fourth cycle ($\theta = \pi/12$, lower level detected).

Even though $\eta \approx 0.1$ and $\langle n\rangle = 5$, we use in all numerical simulations the expression for Ω_n given by Eq. (13), so that corrections of higher order in $\eta^2 n$ are fully taken into account.

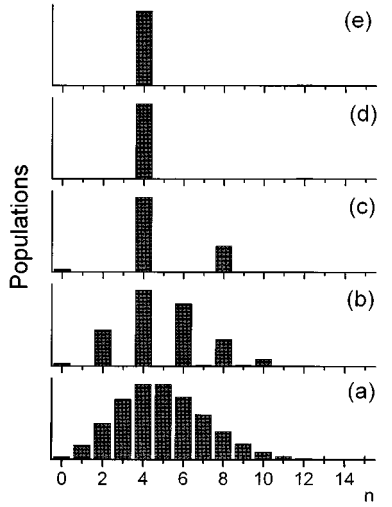

FIG. 4. Population distributions as a function of the vibronic excitation number, for $\Phi_0 = 48\pi$ and $\theta = \pi/2$ in the first cycle (Lamb-Dicke parameter $\eta \approx 0.102$: (a) for an initial coherent state with $\langle n\rangle = 5$; (b) after the first cycle ($\theta = \pi/2$, lower level detected); (c) after the second cycle ($\theta = \pi/4$, lower level detected); (d) after the third cycle ($\theta = \pi/8$, upper level detected); (e) after the fourth cycle ($\theta = \pi/12$, lower level detected).

V. GENERATION OF SCHRÖDINGER CATS

If the initial vibrational state is coherent, so that $c_n = \exp(-|\alpha|^2/2)\alpha^n/\sqrt{n!}$, it follows from Eqs. (23) and (19) that

$$|\Psi(t)\rangle = \frac{1}{\mathcal{N}}[|\alpha e^{-i\theta}\rangle + e^{-i(\Omega_0\tau-\theta)}|\alpha e^{i\theta}\rangle], \qquad (27)$$

where as before $\theta = \eta^2\Omega_0\tau/2$, and the normalization constant is given by

$$\mathcal{N}^2 = 2[1+\cos(|\alpha|^2\sin 2\theta - \Omega_0\tau + \theta)] \times \exp[-|\alpha|^2(1-\cos 2\theta)]. \qquad (28)$$

For $|\alpha|^2 \gg 1$, and θ sufficiently large (e.g., $\theta = \pi/2$), Eq. (27) provides an example of a quantum superposition of distinct coherent states, which is sometimes called a ''Schrödinger cat'' state [12]. In fact, Fig. 4(b) displays a quite characteristic feature of these states: the rapid oscillations in the distribution for the occupation number n [12].

It should be noticed that this state is obtained here at the end of a single cycle, involving therefore a simpler procedure than the one adopted in Ref. [34], at the expense, however, of requiring a greater degree of precision in the definition of the area of the carrier pulse.

VI. CONCLUSIONS

We have shown that it is possible to realize a quantum nondemolition measurement of the vibrational populations of a trapped ion, by means of a sequence of Raman pulses which induce resonant transitions between two electronic states (usually ground-state hyperfine sublevels). The crucial point in this scheme is the dependence of the Rabi oscillations between the two levels on the vibronic quantum number n. For properly chosen parameters, a ''Schrödinger cat'' state is produced after the first pulse and subsequent atomic state detection. Repetition of this cycle leads, for an appropriate choice of pulse areas, to a Fock state. Of course, this scheme is QND so far as the occupation numbers are concerned. Thus, if one starts with a given coherent state, its phase will be quickly randomized by the measurement procedure [one should note that after the first measurement one gets already a superposition of two coherent states with different phases, cf. Eq. (27)]. Equation (19) shows, however, that the measuring process does not spoil the relative phase between the surviving Fock-state components of the original state.

A feedback procedure, by which the areas of successive pulses are chosen according to the result of the atomic state detection in the previous cycle, greatly speeds up the process of getting a Fock state. The whole procedure can be considered as a paradigm of quantum measurement, leading after some time to an eigenvector of the observable being measured, in this case the number of excitations in a vibronic mode.

Note added in proof: Recently, a paper containing similar ideas was published by R. L. de Matos Filho and W. Vogel in Phys. Rev. Lett. **76**, 4520 (1996).

ACKNOWLEDGMENTS

This work was partially supported by the Chilean Consejo Nacional de Investigaciones Cientificas y Tecnológicas (CONICYT), Fundacion Andes, and the Brazilian Conselho Nacional de Desenvolvimento Científico e Tecnológico (CNPq). Two of the authors (L.D. and N.Z.) would like to thank Professor Miguel Orszag and the Facultad de Física of the Pontificia Universidad Católica de Chile for their hospitality.

[1] W. Neuhauser, H. G. Dehmelt, and P. E. Toschek, Phys. Rev. A **22**, 1137 (1980).

[2] F. Diedrich, J.C. Bergquist, W.M. Itano, and D.J. Wineland, Phys. Rev. Lett. **62**, 403 (1989).

[3] P. Verkerk, B. Lounis, C. Salomon, and C. Cohen-Tannoudji, Phys. Rev. Lett. **68**, 3861 (1992); P.S. Jessen, C. Gerz, P.D. Lett, W.D. Phillips, S.L. Rolston, R.J.L. Spreeuw, and C.I. Westbrook, *ibid.* **69**, 49 (1992); A. Hemmerich and T.W. Hänsch, *ibid.* **70** , 410 (1993); G. Grynberg, B. Lounis, P. Verkerk, J.-Y. Courtois, and C. Salomon, *ibid.* **70**, 2249 (1993).

[4] A. Aspect, E. Arimondo, R. Kaiser, N. Vansteenkiste, and C. Cohen-Tannoudji, Phys. Rev. Lett. **61**, 826 (1988); J. Lawall, F. Bardou, B. Saubamea, M. Leduc, A. Aspect, and C. Cohen-Tannoudji, *ibid.* **73**, 1915 (1994); H. Lee, C. Adams, N. Davidson, B. Young, M. Weitz, M. Kasevich, and S. Chu, in *Atomic Physics XIV*, edited by D.J. Wineland, C.E. Wieman, and S.J. Smith (AIP Press, New York, 1995), p. 258.

[5] M. Kasevich and S. Chu, Phys. Rev. Lett. **69**, 1741 (1992).

[6] S. Haroche, in *Fundamental Systems in Quantum Optics*, Proceedings of the Les Houches Summer School of Theoretical Physics, Session LIII, Les Houches, France, 1990, edited by J. Dalibard, J.M. Raimond, and J. Zinn-Justin (Elsevier, Amsterdam, 1992).

[7] E.T. Jaynes and C.W. Cummings, Proc. IEEE **51**, 89 (1963).

[8] C.A. Blockley, D.F. Walls, and H. Risken, Europhys. Lett. **77**, 509 (1992).

[9] H.J. Kimble, in *Fundamental Systems in Quantum Optics* (Ref. [6]), p. 545.

[10] R.J. Thompson, G. Rempe, and H.J. Kimble, Phys. Rev. Lett. **68**, 1132 (1992).

[11] M. Brune, P. Nussenzveig, F. Schmidt-Kaler, F. Bernardot, A. Maali, J.M. Raimond, and S. Haroche, Phys. Rev. Lett. **72**, 3339 (1994).

[12] M. Brune, S. Haroche, V. Lefèvre, J.M. Raimond, and N. Zagury, Phys. Rev. Lett. **65**, 976 (1990); M. Brune, S. Haroche, J.M. Raimond, L. Davidovich, and N. Zagury, Phys. Rev. A **45**, 5193 (1992).

[13] G. Raithel, C. Wagner, W. Walther, L. Narducci, and M. O. Scully, in *Advances in Atomic, Molecular and Optical Physics, Supplement 2* (Academic Press, New York, 1994), p. 57.

[14] W. Nagourney, J. Sandberg, and H.G. Dehmelt, Phys. Rev. Lett. **56**, 2797 (1986); Th. Sauter, W. Neuhauser, R. Blatt, and P.E. Toschek, *ibid.* **57**, 1696 (1986); J.C. Bergquist, R.G. Hu-

let, W.M. Itano, and D.J. Wineland, *ibid.* **57**, 1699 (1986).
[15] D.J. Heinzen and D.J. Wineland, Phys. Rev. A **42**, 2977 (1990).
[16] C. Monroe, D.M. Meekhof, B.E. King, S.R. Jefferts, W.M. Itano, D.J. Wineland, and P. Gould, Phys. Rev. Lett. **75**, 4011 (1995).
[17] C. Monroe, D.M. Meekhof, B.E. King, W.M. Itano, and D.J. Wineland, Phys. Rev. Lett. **75**, 4714 (1995).
[18] D.M. Meekhof, C. Monroe, B.E. King, W.M. Itano, and D.J. Wineland, Phys. Rev. Lett. **76**, 1796 (1996).
[19] F. Diedrich and H. Walther, Phys. Rev. Lett. **58**, 203 (1987); M. Schubert, I. Siemers, R. Blatt, W. Neuhauser, and P.E. Toschek, *ibid.* **68**, 3016 (1992). The first observation of antibunching in resonance fluorescence from an atomic beam was made by H.J. Kimble, M. Dagenais, and L.Mandel, *ibid.* **39**, 691 (1977); observation of sub-Poissonian behavior in the same system was reported by R. Short and L. Mandel, *ibid.* **51** , 384 (1983).
[20] W.M. Itano, D.J. Heinzen, J.J. Bollinger, and D.J. Wineland, Phys. Rev. A **41**, 2295 (1990).
[21] J.I. Cirac and P. Zoller, Phys. Rev. Lett. **74**, 4091 (1995).
[22] W. Jhe, A. Anderson, E.A. Hinds, D. Meschede, L. Moi, and S. Haroche, Phys. Rev. Lett. **58**, 666 (1987); see also S. Haroche and D. Kleppner, Phys. Today **42**, 24 (1989).
[23] G. Rempe and H. Walther, Phys. Rev. Lett. **58**, 353 (1987).
[24] J.I. Cirac, R. Blatt, A.S. Parkins, and P. Zoller, Phys. Rev. Lett. **70**, 762 (1993); J.I. Cirac, R. Blatt, and P. Zoller, Phys. Rev. A **49**, R3174 (1994); R. Blatt, J.I. Cirac, and P. Zoller, *ibid.* **52**, 518 (1995).
[25] J.I. Cirac, A.S. Parkins, R. Blatt, and P. Zoller, Phys. Rev. Lett. **70**, 556 (1993).
[26] B. Baseia, R. Vyas, and V.S. Bagnato, Quantum Opt. **5**, 155 (1993).
[27] D.J. Wineland, J.J. Bollinger, W.M. Itano, F.L. Moore, and D.J. Heinzen, Phys. Rev. A **46**, R6797 (1992); D.J. Wineland, J.J. Bollinger, W.M. Itano, and D.J. Heinzen, *ibid.* **50**, 67 (1994).
[28] V.B. Braginsky, Y.I. Vorontsov, and F.I. Khalili, Zh. Éksp. Teor. Fiz. **73**, 1340 (1977) [Sov. Phys. JETP **46**, 705 (1977)]; W.G. Unruh, Phys. Rev. D **18**, 1764 (1978); V.B. Braginsky and F.I. Khalili, Zh. Éksp. Teor. Fiz. **78**, 1712 (1980) [Sov. Phys. JETP **51**, 859 (1980)]; G.J. Milburn and D.F. Walls, Phys. Rev. A **28**, 2065 (1980); N. Imoto, H. Haus, and Y. Yamamoto, *ibid.* **32**, 2287 (1985).
[29] A.O. Caldeira and A.J. Legett, Phys. Rev. A **31**, 1059 (1985); W. Zurek, Phys. Rev. D **24**, 1516 (1986); W. Zurek, Phys. Today **44**(10), 36 (1991).
[30] L. Davidovich, A. Maali, M. Brune, J.M. Raimond, and S. Haroche, Phys. Rev. Lett. **71**, 2360 (1993); L. Davidovich, M. Brune, J.M. Raimond, and S. Haroche, Phys. Rev. A **53**, 1295 (1996).
[31] J. Von Neumann, *Die Mathematische Grundlagen der Quantenmechanik* (Springer-Verlag, Berlin, 1932); English translation by R.T. Beyer, *Mathematical Foundations of Quantum Mechanics* (Princeton University Press, Princeton, NJ, 1955); K. Hepp, Helv. Phys. Acta **45**, 237 (1972); K. Hepp and E.H. Lieb, *ibid.* **46**, 573 (1973); J.S. Bell, *ibid.* **48**, 93 (1975); see also *Quantum Theory and Measurement*, edited by J.A. Wheeler and W. Zurek (Princeton Univ. Press, Princeton, 1983).
[32] M.D. Levenson, R.M. Shelby, M. Reid, and D.F. Walls, Phys. Rev. Lett. **57**, 2473 (1986); N. Imoto, S. Watkins, and Y. Sasaki, Opt. Commun. **61**, 159 (1987); A. LaPorta, R.E. Slusher, and B. Yurke, Phys. Rev. Lett. **62**, 28 (1989); P. Grangier, J.F. Roch, and G. Roger, *ibid.* **66**, 1418 (1991).
[33] Wolfgang Paul, Rev. Mod. Phys. **62**, 531 (1990).
[34] C. Monroe, D.M. Meekhof, B.E. King, and D.J. Wineland, Science **272**, 1131 (1996).
[35] Although the usual statement of the Lamb-Dicke limit involves only the Lamb-Dicke constant η, which is assumed to be much smaller than 1, it is clear that the stronger condition $\eta\sqrt{n}\ll 1$ is necessary, in general.
[36] W. Vogel and R.L. de Matos Filho, Phys. Rev. A **52**, 4214 (1995).
[37] S. Haroche, M. Brune, and J.M. Raimond, J. Phys. (France) II **2**, 659 (1992).